Mathematical Biosciences and Engineering

MBE, 18(4): 4817–4833.
DOI: 10.3934/mbe.2021245
Received: 15 April 2021
Accepted: 26 May 2021
Published: 02 June 2021

http://www.aimspress.com/journal/MBE

Research article

Effects of thermal slip and chemical reaction on free convective nanofluid from a horizontal plate embedded in a porous media

Abdulaziz Alsenafi[1,*] and M. Ferdows[2]

[1] Department of Mathematics, Kuwait University, Kuwait
[2] Research Group of Fluid Flow Modeling and Simulation, Department of Applied Mathematics, University of Dhaka, Bangladesh

*** Correspondence:** Email: abdulaziz.alsenafi@ku.edu.kw.

Abstract: We consider a two-dimensional, uniform, incompressible and free convection flow of a nano-fluid along a plane. The plate is located facing upward about the porous medium. Throughout the investigation, thermal slip, chemical reaction, heat emission/absorption is considered. In the modeling of nano-fluid we have considered the dynamic effect along with the Brownian and thermophoresis. In obtaining the governing equations, including the boundary conditions, an appropriate scaling is applied. The governing momentum equations, including thermal energy and nanoparticles equations are translated into a group of nonlinear ODEs by using Lie symmetry group transformation. The transformed equations are then solved numerically using the Runge-Kutta-Fehlberg fourth-fifth order. The numerical results of velocity, temperature, and nanoparticle volume fraction profiles for varied physical parameters will be discussed and analyzed at the end. The discussion also includes the local Nusselt and the local Sherwood numbers against several of the systems' physical parameters. It is found that the velocity and temperature decrease with thermal slip and heat absorption whilst it increases by increasing heat generation and chemical reaction order. Our present results will be compared with similar existing literature results.

Keywords: scaling group transformations; nano-fluid; thermal slip; chemical reaction

1. Introduction

Numerous studies were made on convective flow in porous medium owing to its far-reaching applications. Furthermore, in recent years some of the convective flow in porous media applications have been intensively studied due to its wide applications in engineering. For example, they are applied in the energy sectors, in which they are used in post-accidental heat removal in nuclear reactors,

underground disposal of radioactive waste, solar collectors, and oil recovery [1–4]. Other applications include but are not limited to food processing, fibrous insulation, building construction, and nano-based thermal insulation for energy-efficient buildings [5–8]. The fluids containing the solid nanometer-sized (with length scales of 1–10 nm) particles dispersed in some basic fluid that conventionally transfer heat are defined as "nano-fluid". Due to these nanoparticles' thermal conductivity along with the coefficient of heat transfer of the base fluid remarkably increases.

Heat transfer fluids such as synthetic oil, ethylene glycol, and water have a low thermal conductivity [9]. Furthermore, thermal conductivity affects the heat transfer factor across the space spreading the heat transfer medium. In [9], Choi first presented the novel idea of jumbling metallic nanoparticles with non-metallic nanoparticles to a base fluid. The author reported several potential advantages to his idea, such as the rise of heat conveyance and having a smaller heat conveyance size. Choi et al. [10] were from the first to use the term "nano-fluid", and they proved that thermal conductivity augments with the inclusion of small nanoparticles less than 1% by volume. Many researchers [11–13] demonstrated that nano-fluids contain effective thermal conductivity to a great extent compared to base fluids. Consequently, such fluids have an excellent prospective for heat transfer enhancement. In [14], Ghasemi and Aminossadati analyzed natural convection heat transfer in a compound, placed at an inclined position, filled with a CuO/water nano-fluid. Their analysis points out that the inclusion of nanoparticles into pure water shows better performance for heat transfer. Recently, Godson et al. [15] presented an overview of the increase of heat transfer by using nano-fluids.

Various science and engineering studies show the occurrence of heat transfer in porous media of having a saturation of a nano-fluid along with a chemical reaction. On account of these occurrences, nano-fluids are extremely important to both scientists and engineers from the point of practical applications. Several industries make use of this type of flow. Moreover, various engineering applications such as safety measures of a radioactive reactor, combustion systems, solar thermal collectors, metallurgical processes, and chemical engineering contain many transport processes. Thermal and mass diffusion exerts a buoyancy force used by the transport processes of such engineering applications in conducting their working principle. All these processes are run under the effects of a chemical reaction. The convection in a horizontally placed layer with a porous medium was analyzed by Nield and Kuznetsov [16,17], and also in [18] by Cheng and Minkowycz. The aforementioned authors considered a porous medium saturated by nano-fluid. Gorla and Chamkha [19] investigated a porous medium with a nano-fluid saturation with natural convection along an isothermal horizontal plate in the medium.

Hamad et al. [20] have endeavored to deduce the similarity solutions of the flow of a 2-D laminar forced convection past a stretching permeable sheet within a porous medium, assuming a saturation of a nano-fluid in the medium. Recently, Ahmad and Pop [21] have used the nano-fluid model to research the steady mixed convection boundary layer flow along a firmly fixed plane surface placed vertically and surrounded in a porous medium containing a nano-fluid. Lately, an investigation was made by Arifin et al. [22] on the steady free as well as mixed convection boundary layer flow along a plane plate placed horizontally. They assumed the plate was inserted in a porous medium containing a saturation of a nano-fluid. The similarity solutions reduce the free variables of their problem, due to which such solutions are quite widely used. Derivation of all group-invariant similarity solutions of 2-D laminar boundary-layer equations is accomplished by applying Lie group transformations. However, at present, it is widely familiar that the classical Lie symmetry technique is applicable for obtaining similarity solutions, see Ovsiannikov [23], Ibragimov [24], and Bluman [25] et al.

In [26], Krishna et al. investigated the magneto-hydrodynamic convection flow of an electrically conducting viscous incompressible and heat-absorbing fluid through a porous medium over a vertical flat plate under the influence of a magnetic field. In addition, other heat transfers and flow problems on magneto-hydrodynamic nano-fluid with the effect of Hall and ion slip with infinite vertical plate embedded in a porous medium have been studied and analyzed mathematically, among others, by Krishna and his collaborators [27–31]. In [32], Patil et al. investigated the Prandtl magneto-hydrodynamic nanofluid aspects over a stretched sheet with convective boundary conditions.

Different works, such as those in [33–36], use the group method to solve various transport problems. For example, Patil et al. [37] studied the unsteady magneto-hydrodynamic flow of a nano Powell-Eyring fluid near a stagnation point past a convectively heated stretching sheet with thermal radiation and a chemical reaction. The authors used theoretical group analysis to transfer the system of nonlinear PDEs into a system of nonlinear ODE's, which was then solved numerically. Affify and Elgazery [38] used scaling group transformations to study a steady two-dimensional stagnation point flow of heat and mass transfer over a heated porous stretching sheet embedded in a porous medium in the presence of a chemical reaction, with heat generation and absorption effects. Ferdows et al. [39] investigated such merged impacts on uniform MHD free convection flow that transfers mass as well as heat along a vertically stretched flat surface in motion. They considered the moving stretching surface to be permeable.

In [40], Uddin et al. studied the problem of a free convective boundary layer flow of a nano-fluid past a horizontal plate that is placed in a porous media. They considered convective boundary conditions along with suctions and injection at the wall. In [41], the authors investigated the amalgamated effects of convective surface boundary conditions along with thermal radiation. The effects were studied on a uniform magneto-hydrodynamic free convection flow that transfers heat and mass along a vertically stretched flat surface. In their investigation, the authors assumed that the permeable stretching surface was in motion. Thermal radiation and a convective surface boundary condition have a plethora of effects on fluid flow. Rashidi et al. [42] used optimal homotopy analysis to study the laminar incompressible free convection flow of a nano-fluid past a chemically reacted plate that is placed in a porous medium. The boundary conditions were considered to be convective along with suction and injection at the wall.

The influence of thermal slip boundary condition with chemical reaction and heat emission/absorption on free convection nano-fluid past a horizontal plate in porous media with free stream conditions has not been mentioned in the literature. Our present study aims to investigate the consequences of thermophoresis, Brownian motion, thermal slip, chemical reaction, and heat emission/absorption on the boundary layer flow of a nano-fluid. The flow is considered along a horizontal plate at an upward-facing position. The entire investigation is conducted to obtain the results numerically. The governing equations are translated into a group of nonlinear ODEs by using Lie symmetry group transformation. The corresponding boundary conditions are also analyzed. Finally, graphical analysis is presented on the resulting consequences of governing parameters on the dimensionless flow profiles.

This paper's outline is as follows: In Section 2, we formulate our model. In Section 3, we perform the Lie group analysis. After that, in Section 4, we discuss our physical quantities and the non-dimensional quantities. Then, in Sections 5 and 6, we present the results of our model simulations as well as show our analysis. Finally, in section 7, we conclude with a discussion of our results.

2. Problem formulation

In this problem, we consider a laminar, 2-D free convective boundary layer flow of a nano-fluid. The nano-fluid is assumed to flow over a horizontally placed plate upwardly faced and held in a Darcy porous medium. We select a coordinate frame in which the x-axis is in the horizontal direction, and the y-axis is normal to it (Figure 1). Across the space separating the constitute of the plate and the fluid, a chemical reaction of order n occurs. This chemical reaction is assumed to be homogeneous, isothermal, and reversible. On the surface, the fraction volume of the nanoparticle (C) and the temperature (T) are assumed to be constants and take the values C_W and T_W, respectively. We denote the corresponding values of T and C as obtained at free stream by T_∞ and C_∞, respectively. As in [43], we also assume that $T_W > T_\infty$, and that the Boussinesq-approximation is used.
The following assumptions are considered:

- At the boundaries, it is assumed that $T = T_w$ and $C = C_w$ are both constants.
- The corresponding values of T and C as obtained at free stream are denoted by T_∞ and C_∞, respectively.
- It is assumed that $T_w > T_\infty$.
- It is assumed that the Boussinesq approximation is used.

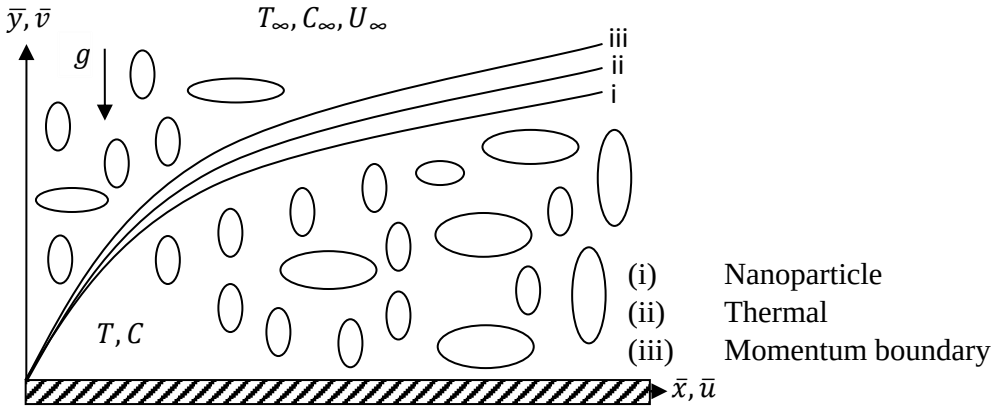

Figure 1. Flow model along with the coordinate system.

As in references [41–44], the conservation of mass, momentum, energy, and properties of the nanoparticles are respectively described by the following four field equations:

$$\nabla \cdot \vec{V} = 0, \tag{1}$$

$$\frac{\rho_f}{\epsilon}\frac{\partial \vec{V}}{\partial t} = -\nabla P - \frac{\mu}{K}\vec{V} + \left[C\rho_P + (1-C)\left(\rho_f\left(1-\beta(T-T_\infty)\right)\right)\right]\vec{g}, \tag{2}$$

$$\frac{\partial T}{\partial t} + \vec{V}\cdot\nabla T = k_m\nabla^2 T + \tau\left[D_B\nabla C\cdot\nabla T + \left(\frac{D_T}{T_\infty}\right)\nabla T\cdot\nabla T\right] + \dot{q}, \tag{3}$$

$$\frac{\partial C}{\partial t} + \vec{V}\cdot\nabla C = D_B\nabla^2 C + \left(\frac{D_T}{T_\infty}\right)\nabla^2 T - k(\bar{x})(C-C_\infty)^n. \tag{4}$$

In the equations above, $\vec{V} = (\bar{u}, \bar{v})$, and $\tau = \frac{(\rho c_P)_P}{(\rho c_P)_f}$. Also, the thermophoretic diffusion coefficient is denoted by D_T is, the Brownian motion diffusion coefficient is denoted by D_B , the porous media

porosity is denoted by ϵ, and finally, $(\rho C)_f$ and $(\rho C)_P$ denote the heat capacity of our fluid and nanoparticles, respectively. We assumed that we have a slow flow ignoring an advective term quadratic drag by Buongiorno [45] and Nield and Kuznetsov [46]. The momentum equation is linearized by assuming nanoparticle concentration is diluted with a befitting selection for the reference pressure. Thus, Eq (2) corresponds to the following form:

$$-\nabla P - \frac{\mu}{k_1}\vec{V} + \left[\left(\rho_P - \rho_{f_\infty}\right)(C - C_\infty) + (1 - C_\infty)\rho_{f_\infty}\beta(T - T_\infty)\right]\vec{g} = 0, \tag{5}$$

where ρ_P and ρ_f are the density of particles and base fluid, respectively.

The effect of volumetric heat generation as a function of temperature in the flow region is given by:

$$\dot{q} = \frac{Ra^{2/3}Q_0}{L^{4/3}\bar{x}^{4/3}}(T - T_\infty), \qquad T > T_\infty, \tag{6}$$

where Q_0 is the heat constant, and L is assumed to be the length of our plate. The reaction rate also varies as the following function:

$$k(\bar{x}) = \frac{Ra^{2/3}k_0}{L^{4/3}\bar{x}^{4/3}}, \tag{7}$$

where k_0 denotes the constant reaction rate.

Considering the previous suppositions, and following references [41–44], the governing equations are rewritten as:

$$\frac{\partial \bar{u}}{\partial \bar{x}} + \frac{\partial \bar{v}}{\partial \bar{y}} = 0, \tag{8}$$

$$\frac{\partial P}{\partial \bar{x}} = -\frac{\mu}{k_1}\bar{u}, \tag{9}$$

$$\frac{\partial P}{\partial \bar{y}} = -\frac{\mu}{K}\bar{v} \pm \left[(1 - C_\infty)\rho_{f_\infty} g\beta(T - T_\infty) - \left(\rho_P - \rho_{f_\infty}\right)g(C - C_\infty)\right], \tag{10}$$

$$\bar{u}\frac{\partial T}{\partial \bar{x}} + \bar{v}\frac{\partial T}{\partial \bar{y}} = \alpha_m \frac{\partial^2 T}{\partial \bar{y}^2} + \tau\left[D_B\frac{\partial C}{\partial \bar{y}}\frac{\partial T}{\partial \bar{y}} + \left(\frac{D_T}{T_\infty}\right)\left(\frac{\partial T}{\partial \bar{y}}\right)^2\right] + \frac{Q_o}{(\rho C)_f}\frac{\mathrm{Ra}^{2/3}}{L^{4/3}\bar{x}^{4/3}}(T - T_\infty), \tag{11}$$

$$\bar{u}\frac{\partial C}{\partial \bar{x}} + \bar{v}\frac{\partial C}{\partial \bar{y}} = D_B\frac{\partial^2 C}{\partial \bar{y}^2} + \left(\frac{D_T}{T_\infty}\right)\frac{\partial^2 T}{\partial \bar{y}^2} - \frac{\mathrm{Ra}^{2/3}k_0}{L^{4/3}\bar{x}^{4/3}}(C - C_\infty)^n, \tag{12}$$

where $\alpha_m = \frac{k_m}{(\rho c_P)_f}$ is the thermal diffusivity, k_m is the thermal conductivity, the parameter $\tau = \frac{\epsilon(\rho C)_p}{(\rho C)_f}$, and the boundary conditions take the form:

$$\begin{aligned} &\bar{v} = 0, \qquad T = T_w + D_1\frac{\partial T}{\partial \bar{y}}, \qquad C = C_w \quad \text{when} \quad \bar{y} = 0, \\ &\bar{u} \to \bar{U}_\infty, \qquad T \to T_\infty, \qquad C \to C_\infty \quad \text{as} \quad \bar{y} \to \infty. \end{aligned} \tag{13}$$

In Eq (13) above, D_1 is the thermal slip factor, and the studied boundary conditions are different from those in references [41–44].

Now, to transform Eqs (6) to (11), we set:

$$x = \frac{\bar{x}}{L\sqrt{Ra}}, \qquad y = \frac{\bar{y}}{L}, \quad u = \frac{\bar{u}L}{\alpha_m\sqrt{Ra}}, \qquad v = \frac{\bar{v}L}{\alpha_m}, \qquad U_\infty = \frac{\bar{U}_\infty L}{\alpha_m\sqrt{Ra}},$$

$$\theta = \frac{T - T_\infty}{\Delta T}, \qquad \phi = \frac{C - C_\infty}{\Delta C}, \qquad \Delta T = T_w - T_\infty, \qquad \Delta C = C_w - C_\infty. \tag{14}$$

Assuming ψ to be a stream function such that

$$u = \frac{\partial \psi}{\partial y} \text{ and } v = -\frac{\partial \psi}{\partial x}. \tag{15}$$

As in references [40] and [42], we substitute the stream function into Eqs (8)–(13) and further assume that the free stream velocity $U_\infty = x^m$, which gives us:

$$\Delta_1 \equiv \frac{\partial^2 \psi}{\partial y^2} + \frac{\partial \theta}{\partial x} - Nr \frac{\partial \phi}{\partial x} = 0, \tag{16}$$

$$\Delta_2 \equiv \frac{\partial \psi}{\partial y}\frac{\partial \theta}{\partial x} - \frac{\partial \psi}{\partial x}\frac{\partial \theta}{\partial y} - \frac{\partial^2 \theta}{\partial y^2} - Nb\frac{\partial \theta}{\partial y}\frac{\partial \phi}{\partial y} - Nt\left(\frac{\partial \theta}{\partial y}\right)^2 + \frac{Q\theta}{x^{4/3}} = 0, \tag{17}$$

$$\Delta_3 \equiv Le\left[\frac{\partial \psi}{\partial y}\frac{\partial \phi}{\partial x} - \frac{\partial \psi}{\partial x}\frac{\partial \phi}{\partial y}\right] - \frac{\partial^2 \phi}{\partial y^2} - \frac{Nt}{Nb}\frac{\partial^2 \theta}{\partial y^2} - \frac{K\phi^n}{x^{4/3}} = 0. \tag{18}$$

The boundary conditions in Eq (13) are transformed to:

$$\begin{aligned} &\frac{\partial \psi}{\partial x} = 0, \qquad \theta = 1 + \frac{D_1}{L}\frac{\partial \theta}{\partial y}, \qquad \phi = 1 \quad \text{at} \quad y = 0, \\ &\frac{\partial \psi}{\partial y} \to x^m, \qquad \theta \to 0, \qquad \phi \to 0 \quad \text{as} \quad y \to \infty. \end{aligned} \tag{19}$$

The parameters in Eqs (16)–(18) are Nt (thermophoresis), Nb (Brownian motion), Nr (buoyancy ratio), Q (heat generation), K (chemical reaction), and Le (Lewis number). Now, similar to Tapanidis et al. [47], we define our parameters as

$$\begin{aligned} Nt = \frac{\tau D_T \Delta T}{\alpha_m T_\infty}, \qquad Nb = \frac{\tau D_B \Delta C}{\alpha_m}, \qquad Nr = \frac{(\rho_P - \rho_{f\infty})\Delta C}{\rho_{f\infty}\beta(1 - C_\infty)\Delta T} \\ Q = \frac{Q_0 L^2}{\alpha_m (\rho \mathrm{C})_f}, \qquad K = \frac{k_0 L^2 (\Delta \mathrm{C})^{n-1}}{\alpha_m}, \qquad Le = \frac{\alpha_m}{D_b} \end{aligned} \tag{20}$$

3. Lie group analysis

Scaling group transformations are a distinctive case of Lie group analysis [46,47]. We consider the following:

$$\Gamma : x^* = x e^{\epsilon \alpha_1}, \; y^* = y e^{\epsilon \alpha_2}, \; \psi^* = \psi e^{\epsilon \alpha_3}, \; \theta^* = \theta e^{\epsilon \alpha_4}, \; \phi^* = \phi e^{\epsilon \alpha_5}, \; D_1^* = D_1 e^{\epsilon \alpha_6}. \tag{21}$$

In the above equation, ϵ is the parameter of group Γ, and α_i $(i = 1, 2, \ldots, 6)$ are assumed to be real numbers. The transformations in Eq (21) can be considered as a point transformation that converts the coordinates from $(x, y, \psi, \theta, \phi, D_1)$ into $(x^*, y^*, \psi^*, \theta^*, \phi^*, D_1^*)$. Now, we find the relation between α_i such that

$$\Delta_j\left(x^*, y^*, \theta^*, \varphi^*, \cdots, \frac{\partial^3 \psi^*}{\partial y^{*3}}\right) = H_j\left(x, y, \theta, \phi, \cdots, \frac{\partial^3 \psi}{\partial y^3}; a\right)\Delta_j\left(x, y, \theta, \phi, \cdots, \frac{\partial^3 \psi}{\partial y^3}\right), \tag{22}$$

where $j = 1, 2, 3$.

The differential forms $\Delta_1, \Delta_2,$ and Δ_3 are required to be conformally constant under group transformation in Eq (21). As done in references [48–50], we set the conversions in Eq (21) into Eqs (16)–(18) to give us the following:

$$\Delta_1 \equiv \frac{\partial^2\psi^*}{\partial y^{*2}} + \frac{\partial\theta^*}{\partial x^*} - Nr\frac{\partial\phi^*}{\partial x^*}$$
$$= e^{\epsilon(\alpha_3-2\alpha_2)}\frac{\partial^2\psi}{\partial y^2} + e^{\epsilon(\alpha_4-\alpha_1)}\frac{\partial\theta}{\partial x} - e^{\epsilon(\alpha_5-\alpha_1)}\frac{\partial\phi}{\partial x}, \tag{23}$$

$$\Delta_2 \equiv \frac{\partial\psi^*}{\partial y^*}\frac{\partial\theta^*}{\partial x^*} - \frac{\partial\psi^*}{\partial x^*}\frac{\partial\theta^*}{\partial y^*} - \frac{\partial^2\theta^*}{\partial y^{*2}} - Nb\frac{\partial\theta^*}{\partial y^*}\frac{\partial\phi^*}{\partial y^*} - Nt\left(\frac{\partial\theta^*}{\partial y^*}\right)^2 + \frac{Q\theta^*}{x^{*4/3}}$$
$$= e^{\epsilon(\alpha_3+\alpha_4-\alpha_1-\alpha_2)}\left[\frac{\partial\psi}{\partial y}\frac{\partial\theta}{\partial x} - \frac{\partial\psi}{\partial x}\frac{\partial\theta}{\partial y}\right] - e^{\epsilon(\alpha_4-2\alpha_2)}\frac{\partial^2\theta}{\partial y^2}$$
$$- e^{\epsilon(\alpha_4+\alpha_5-2\alpha_2)}Nb\frac{\partial\theta}{\partial y}\frac{\partial\phi}{\partial y} - e^{\epsilon(2\alpha_4-2\alpha_2)}Nt\left(\frac{\partial\theta}{\partial y}\right)^2 + e^{\epsilon\left(\alpha_4-\frac{4}{3}\alpha_1\right)}\frac{Q\theta}{x^{4/3}}, \tag{24}$$

$$\Delta_3 \equiv Le\left[\frac{\partial\psi^*}{\partial y^*}\frac{\partial\phi^*}{\partial x^*} - \frac{\partial\psi^*}{\partial x^*}\frac{\partial\phi^*}{\partial y^*}\right] - \frac{\partial^2\phi^*}{\partial y^{*2}} - \frac{Nt}{Nb}\frac{\partial^2\theta^*}{\partial y^{*2}} - \frac{K\phi^*}{x^{*4/3}}$$
$$= -e^{\epsilon(\alpha_5-2\alpha_2)}\frac{\partial^2\phi}{\partial y^2} + e^{\epsilon(\alpha_3+\alpha_5-\alpha_1-\alpha_2)}Le\left[\frac{\partial\psi}{\partial y}\frac{\partial\phi}{\partial x} - \frac{\partial\psi}{\partial x}\frac{\partial\phi}{\partial y}\right]$$
$$-e^{\epsilon(\alpha_4-2\alpha_2)}\frac{Nt}{Nb}\frac{\partial^2\theta}{\partial y^2} - e^{\epsilon\left(\alpha_5-\frac{4}{3}\alpha_1\right)}\frac{K\phi^n}{x^{4/3}}. \tag{25}$$

The invariance under the group Γ is invoked, and from it, we obtain the following relationships:

$$\alpha_3 - 2\alpha_2 = \alpha_4 - \alpha_1 = \alpha_5 - \alpha_1,$$
$$\alpha_3 + \alpha_4 - \alpha_1 - \alpha_2 = \alpha_4 - 2\alpha_2 = \alpha_4 + \alpha_5 - 2\alpha_2 = 2\alpha_4 - 2\alpha_2 = \alpha_4 - \frac{4}{3}\alpha_1,$$
$$\alpha_3 + \alpha_5 - \alpha_1 - \alpha_2 = \alpha_5 - 2\alpha_2 = \alpha_4 - 2\alpha_2 = \alpha_5 - \frac{4}{3}\alpha_1. \tag{26}$$

The boundary conditions yield:

$$\alpha_3 - \alpha_1 = 0, \quad \alpha_4 = 0 = \alpha_4 + \alpha_6 - \alpha_2, \quad \alpha_5 = 0, \quad \alpha_2 - \alpha_3 = -m\alpha_1. \tag{27}$$

Now, solving Eqs (26) and (27) yields

$$\alpha_4 = \alpha_5 = 0, \quad \alpha_1 = \frac{3\alpha_2}{2}, \quad \alpha_3 = \frac{\alpha_2}{2}, \quad \alpha_6 = \alpha_2, \quad \text{and} \quad m = -\frac{1}{3}. \tag{28}$$

The set of transformation under group Γ reduces to

$$x^* = xe^{3\epsilon\alpha_2/2},\ y^* = ye^{\epsilon\alpha_2},\ \psi^* = \psi e^{\epsilon\alpha_2/2},\ \theta^* = \theta,\ \phi^* = \phi,\ D_1^* = D_1e^{\epsilon\alpha_2}. \tag{29}$$

Now, taking Taylor series expansion about ϵ gives us:

$$x^* - x = \frac{3x\epsilon\alpha_2}{2} + O(\epsilon^2), \quad y^* - y = \epsilon\alpha_2 y + O(\epsilon^2), \quad \psi^* - \psi = \frac{\epsilon\psi\alpha_2}{2} + O(\epsilon^2),$$
$$\theta^* - \theta = 0, \quad \phi^* - \phi = 0, \quad D_1^* - D = \epsilon\alpha_2 D_1 + O(\epsilon^2) \tag{30}$$

As $\alpha_2 \neq 0$, we can rewrite the equations above as the following characteristic equations:

$$\frac{2(x^* - x)}{3x\alpha_2} = \epsilon, \quad \frac{y^* - y}{\alpha_2 y} = \epsilon, \quad \frac{2(\psi^* - \psi)}{\psi\alpha_2} = \epsilon, \quad \frac{D_1^* - D}{\alpha_2 D_1} = \epsilon$$

$$\theta^* - \theta = 0, \qquad \phi^* - \phi = 0, \tag{31}$$

Thus, in terms of differentials, we have that:

$$\frac{dy}{\alpha_2 y} = \frac{2dx}{3\alpha_2 x} \tag{32}$$

$$\frac{2d\psi}{\alpha_2 \psi} = \frac{2dx}{3\alpha_2 x} \tag{33}$$

$$\frac{dD_1}{\alpha_2 D_1} = \frac{2dx}{3\alpha_2 x} \tag{34}$$

$$d\theta = d\phi = 0 \tag{35}$$

3.1. Similarity transformations

Now, integrating Eq (32) gives us:

$$yx^{-\frac{2}{3}} = \eta, \tag{36}$$

where η is a constant. Likewise, integrating Eq (33) yields:

$$\psi = x^{\frac{1}{3}} f(\eta), \tag{37}$$

where $f(\eta)$ is a constant, and integrating Eq (34) gives us:

$$D_1 = (D_1)_0 x^{\frac{2}{3}}, \tag{38}$$

where $(D_1)_0$ is a constant. Finally, from Eq (35), we have that:

$$\theta = \theta(\eta) \text{ and } \phi = \phi(\eta) \tag{39}$$

where $\theta(\eta)$ and $\phi(\eta)$ are constants. Therefore, from Eqs (36)–(39), we get that:

$$\eta = yx^{-\frac{2}{3}}, \ \psi = x^{\frac{1}{3}} f(\eta), \ \theta = \theta(\eta), \text{ and } \quad D_1 = (D_1)_0 x^{\frac{2}{3}}. \tag{40}$$

We note that the similarity transformations in Eq (40) are congruous with the conventional similarity transformations as described in Cheng and Chang [51] for λ=0. Thus, the expression of u, v becomes:

$$u = \frac{f'}{x^{1/3}}, \qquad \text{and} \qquad v = -\frac{1}{3x^{2/3}}(f - 2\eta f') \,. \tag{41}$$

3.2. Similarity equations

Making substitution of the transformations in Eq (40) into the governing Eqs (16)–(18) gives us:

$$f'' - \tfrac{2}{3}(\theta' - Nr\phi') = 0, \tag{42}$$

$$\theta'' + \frac{1}{3} f\theta' + Nb\theta'\phi' + Nt(\theta')^2 + Q\theta = 0, \tag{43}$$

$$\theta'' + \frac{Le}{3} f\theta' + \frac{Nt}{Nb}\theta'' - K\phi^n = 0, \tag{44}$$

contingent on the boundary conditions

$$f(0) = 0, \qquad \theta(0) = 1 + b\theta'(0), \qquad \phi(0) = 1,$$

$$f'(\infty) = 1, \qquad \theta(\infty) = 0, \qquad \phi(\infty) = 0, \tag{45}$$

where, $b = (D_1)_0/L$ is the thermal slip parameter.

4. Physical quantities

In our present problem, the parameters of physical significance are the local Nusselt number $Nu_{\bar{x}}$, local skin friction coefficient $C_{f\bar{x}}$, and the local Sherwood number $Sh_{\bar{x}}$, respectively. Physically, $C_{f\bar{x}}$ is the shear stress of the wall, $Nu_{\bar{x}}$ is the rate of transfer of heat in the wall, whilst $Sh_{\bar{x}}$ symbolizes the rate of volume fraction of nanoparticles in the wall. The following relations are applied to obtain the aforementioned quantities:

$$C_{f\bar{x}} = \frac{2\mu}{\rho U_r^2}\left(\frac{\partial \bar{u}}{\partial \bar{y}}\right)_{\bar{y}=0}, \qquad Nu_{\bar{x}} = \frac{-\bar{x}}{T_f - T_\infty}\left(\frac{\partial T}{\partial \bar{y}}\right)_{\bar{y}=0}, \qquad Sh_{\bar{x}} = \frac{-\bar{x}}{C_w - C_\infty}\left(\frac{\partial C}{\partial \bar{y}}\right)_{\bar{y}=0}. \tag{46}$$

Substituting Eqs (12) and (40) into Eq (46) shows that the physical quantities can be written in the following dimensionless form:

$$\frac{1}{2}Ra_{\bar{x}}PrC_{f\bar{x}} = f''(0), \qquad Ra_{\bar{x}}^{-1/3}u_{\bar{x}} = -\theta'(0), \qquad \frac{1}{2}Ra_{\bar{x}}^{-1/3}Sh_{\bar{x}} = -\theta'(0). \tag{47}$$

In the equation above, $Ra_{\bar{x}} = \frac{gK\beta(1-C_\infty)\Delta T\bar{x}}{\alpha_m \nu}$ is the local Rayleigh number, $pr = \frac{\nu}{\alpha_m}$ is the Prandtl number, and $U_r = \frac{(1-C_\infty)gK\beta\Delta T}{\alpha_m}$ is the reference velocity.

5. Numerical solutions

A two-point boundary value problem is formed by the set of coupled nonlinear ODEs in Eq (42) through Eq (44) with the boundary conditions in Eq (45). In [52], Aziz showed numerically using Runge-Kutta-Fehlberg's method in Maple that similarity solutions are possible for convective surface boundary conditions. Moreover, White and Subramanian [53] examined the above process's precision for different transport problems.

A finite value of 10 for the similar variable $\eta_{\max}$ is used to replace the asymptotic boundary conditions given in Eq (43). The chosen value of $\eta_{\max}$ assured the correct mannered approach of all numerical solutions to the far-field asymptotic values, which is often ignored. In [54], Pantokratoras studied convective heat transfer problems, and in his report, he found some erroneous results in the convective heat transfer problems. He identified the reason behind these errors as the graphs for the temperature, velocity, and the volume fraction (concentration) of nanoparticle distributions in the boundary layers do not tend to the accurate values in an asymptotic manner owing to the infinitesimal value of $\eta_{\max}$.

Here we perform numerical computations for $0.1 \le Nb \le 0.5,\ 0.1 \le Nt \le 0.5,\ 0.1 \le Nr \le 0.5,\ 1 \le Le \le 10,\ -0.5 \le Q \le 0.5, 0.5 \le K \le 3, 0 \le b \le 1,$ and $1 \le n \le 3$. At the end of our discussion, we measured the wall shear stress, local heat transfer rate, and local mass transfer rate, respectively, with regard to the local skin friction coefficient, the reduced local Nusselt number Nu, and reduced local Sherwood number Shr. Finally, to evaluate our numerical computations' precision, we compared our results to that of Gorla and Chamkha [19]. Both sets of results are summarized in Table 1, and it is worth noting that we found our results to compare exceptionally well.

We note that when the case when the thermal slip parameter is ($b = 0$), buoyancy force ($Nr = 0$), thermophoresis ($Nt = 0$), heat generation ($Q = 0$), chemical reaction ($k = 0$), and Brownian motion

($Nb \to 0$), our undertaken problem transforms to the problem, which had been inspected by Cheng and Chang [50] for the case of $\lambda = 0$ in their work.

Table 1. Comparison of our results with [19].

	Present results		[19]	
	$-\theta'(0)$	$-\phi'(0)$	$-\theta'(0)$	$-\phi'(0)$
Nr	$Nb = 0.3,\ Nt = 0.1,\ Le = 10,\ b = K = Q = 0$			
0.1	0.325859	1.482246	3.26E-01	1.484164
0.2	0.323929	1.466855	3.25E-01	1.468161
0.3	0.321953	1.451057	3.22E-01	1.452664
Nt	$Nb = 0.3,\ Nr = 0.5,\ Le = 10,\ b = K = Q = 0$			
0.1	0.317842	1.418114	3.19E-01	1.419499
0.2	0.304917	1.414708	3.05E-01	1.416536
0.3	0.292751	1.415425	2.93E-01	1.416866
Nb	$Nt = 0.1,\ Nr = 0.5,\ Le = 10,\ b = K = Q = 0$			
0.1	0.367286	1.325843	3.68E-01	1.327454
0.2	0.342789	1.391928	3.43E-01	1.393615
0.3	0.317842	1.418114	3.19E-01	1.419499

6. Results and discussion

Numerical solution to Eqs (42)–(44) with boundary conditions in Eq (45) is obtained by applying the Runge-Kutta-Fehlberg fourth-fifth order numerical method. We performed the computations using the software Maple 13, and our numerical results are displayed graphically for emphasizing the significant attributes of the flow characteristics.

In Figures 2 and 3, we have presented the velocity profiles within the boundary layer for both thermal slip parameter b, and no-thermal slip parameter ($b = 0$) against several values of heat emission/absorption parameter Q, chemical reaction parameter k, and reaction order n, respectively.

Figure 2(a) shows that the velocity profiles inside the boundary layer become high; hence the boundary layer's thickness rises with the increase of heat generation/absorption parameter Q. As heat evolves, the buoyancy force increases, which in turn causes the flow rate to reduce, which triggers an increase in the velocity profile. However, with the intensification of heat absorption, the velocity is observed to decrease due to the buoyancy force's decrease. Figure 2(b) shows that the velocity profiles $f'(\eta)$ inside the boundary layer increase as the chemical reaction parameter K increase, and the boundary layer's width also decreases. This is because physically, the fluid motion becomes thicker as K increases. In both Figure 2(a),(b), we clearly see that an increase in the thermal slip parameter b causes the velocity profiles $f'(\eta)$ to decrease. Therefore, the velocity profiles increase with the heat generation and order of chemical reaction, while they decrease when the thermal slip increases.

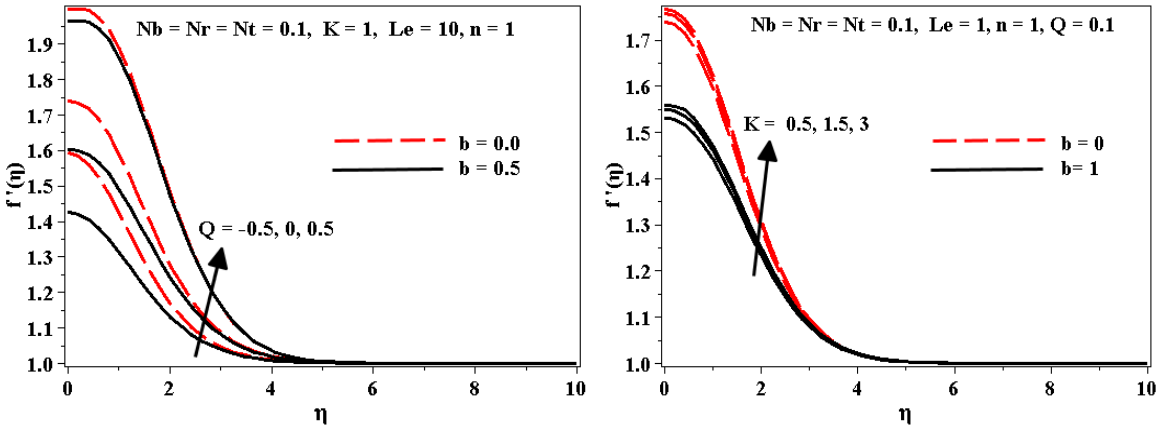

(a) (b)

Figure 2. Effect of the generation and the chemical reaction parameters on the dimensionless velocity profiles for thermal slip parameter.

Figure 3 shows that the velocity profiles $f'(\eta)$ inside the boundary layer slightly expand, and consequently, the width of the boundary layer decrease as the order reaction parameter n rises. As in Figure 2, we see that the velocity profiles decrease as the thermal slip thermal parameter b increases.

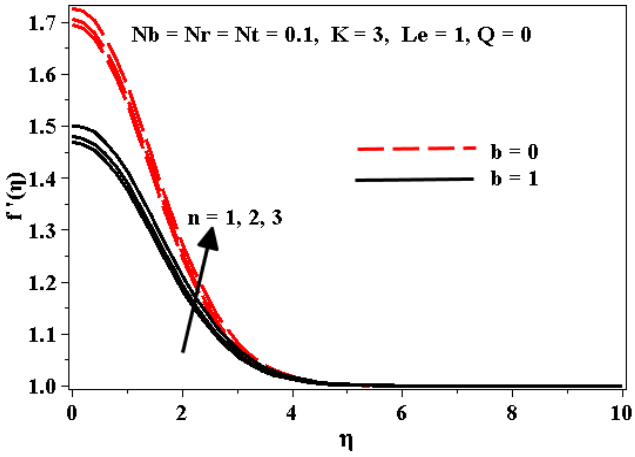

Figure 3. Effect of the order of chemical reaction and the Lewis number on the dimensionless velocity profiles against several thermal slip parameter values.

In Figure 4(a),(b), we have presented the temperature profiles $\theta(\eta)$ within the boundary layer for both thermal slip parameter b and no-thermal slip parameter ($b = 0$) for several values of heat emission/absorption parameter Q, and order of reaction n, respectively. Figure 4(a) displays that the boundary layer's temperature profiles increase; hence, the boundary layer's thickness increases with the heat generation/absorption parameter. As heat generation ($Q > 0$), it is evident that there is a rise in the thermal state of the fluid. As a result, we notice that the temperature enhances as Q attains larger values. However, when heat absorption ($Q < 0$), the exact converse happens, and this result agrees with previous work done by Alsaedi et al. [55]. Figure 4(b) shows that the boundary layer's temperature profiles increase; hence, the boundary layer's width extends as the order reaction parameter n increases. As the thermal slip parameter becomes large, less heat is transferred from the surface to the fluid, and consequently, the temperature profiles decrease.

In Figure 5(a),(b), we have presented the nanoparticle volume fraction profiles $\phi(\eta)$ within the boundary layer for various values of the order of reaction n, Lewis number Le, chemical reaction parameter K, and the thermal slip parameter b, respectively. Figure 5(a) shows that the nanoparticle volume fraction profiles within the boundary layer increase; hence, the boundary layer's width becomes greater as the reaction order becomes large. This is because the Lewis number Le is inversely proportional to the diffusion coefficient. Consequently, a rise in Le yields a reduction in diffusion, which lastly results in a drop in nanoparticle concentration. Figure 5(b) shows that the nanoparticle volume fraction profiles within the boundary layer decrease; hence, the boundary layer's width enhances as the chemical reaction parameter rises. This result agrees with previous work by Abdul-Kahar et al. [35]. For both the "slip thermal" and "no-slip thermal" cases, the nanoparticle volume fraction profiles decrease monotonically as K increases. These physical behaviors are demonstrated because of the coalesced effects of the Brownian motion and thermophoresis particle deposition strength.

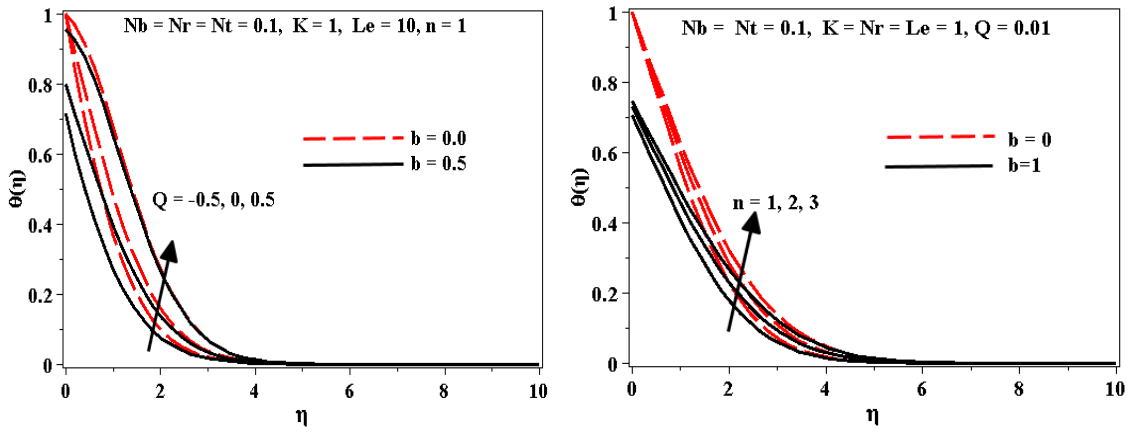

(a) (b)

Figure 4. Effect of the heat generation and the order of chemical reaction on the dimensionless temperature profiles against several thermal slip parameter values.

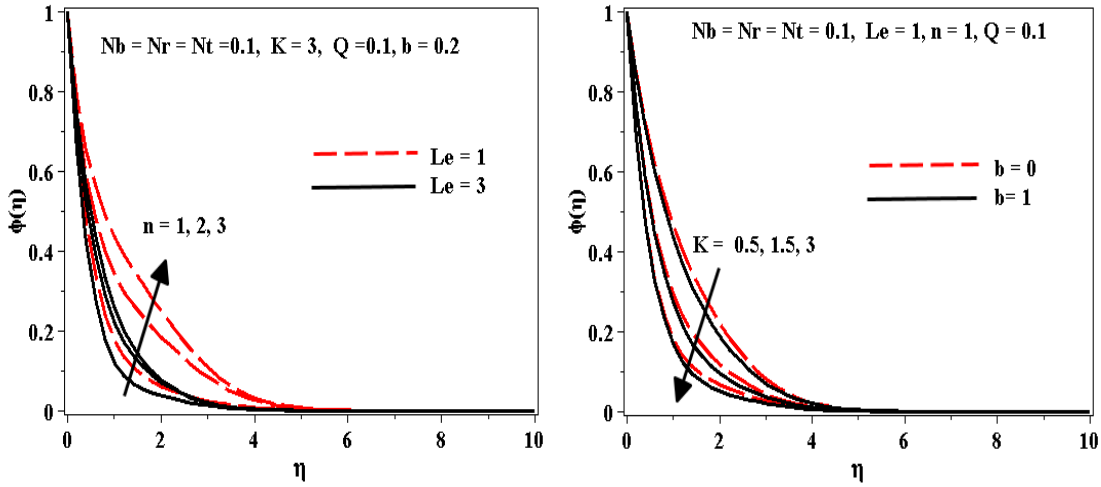

(a) (b)

Figure 5. Effect of the chemical reaction and the order of chemical reaction on the dimensionless concentration profiles against several thermal slip parameter values.

Table 2 shows the effects of thermal slip, order of chemical reaction, reaction rate, and generation parameters on the dimensionless heat and mass transfer rates. In Table 2, we also that the rates of heat and mass transfer decrease as the thermal slip and order of chemical reaction parameters increase. Thus, the generation and reaction parameters reduce with the heat transfer rate whereas, the parameters increase as the mass transfer rate increase. In this respect, let us note that there is a significant effect on the flow field and accordingly on the heat transfer rate and nanoparticle volume fraction from the plate to the fluid. These effects are observed by the impact of thermophoresis particle deposition in the existence of the heat generation, order of chemical reaction, thermal slip, and chemical reaction parameters with Brownian motion. This demonstrates that all the previous parameters will significantly influence the heating and cooling processes in nano-fluids. This work has aided both scientists and engineers understand the most significant working principle of the deposition process.

Table 2. Variation of $-\theta'(0)$ and $-\phi'(0)$ for various parameters values.

b	Q	K	n	$-\theta'(0)$	$-\phi'(0)$
0	0.1	0.1	1	0.44700	1.90384
0.2	0.1	0.1	1	0.40473	1.88000
0.5	0.1	0.1	1	0.35527	1.84997
0.2	0.3	0.1	1	0.26873	2.02794
0.2	0.5	0.1	1	0.09773	2.20642
0.2	0.1	0.2	1	0.40469	1.90508
0.2	0.1	0.4	1	0.40464	1.95445
0.2	0.1	0.1	2	0.40474	1.87060
0.2	0.1	0.1	3	0.40473	1.86665

A vast range of scientific and engineering applications are being extended in fluid mechanics, heat transfer, and nanoparticle volume fraction. Because of this wide-ranged scope, free convective flow through porous media became a great study area undergoing rapid growth in the aforesaid fields. Finally, we mention one promising scientific implementations of nanoparticles, which is the use of heat transfer fluids with the dispersion of nanoparticles to challenge cooling problems in thermal systems.

7. Conclusions

Our present paper includes the numerical and physical study of the 2D steady free convective flow of a nano-fluid. The flow is assumed along with a horizontal plate that is faced upward and saturated in a porous medium. Our study considered thermal slip, chemical reaction, and heat emission/absorption under the Brownian motion and thermophoresis. Applying Lie group analysis, firstly, we observe the symmetries of the basic equations, following which we transform these equations to ODEs. We then worked with the resulting equations to obtain the numerical solution using Runge-Kutta-Fehlberg's fourth-fifth order numerical technique with Maple 13. Finally, to recapitulate our most prominent findings, we can write the following:

1) The velocity decreases as the thermal slip and heat absorption increase whilst it increases as the heat generation, order of chemical reaction, and reaction parameters increase.

2) The temperature decreases as the thermal slip and heat absorption increase, whilst it increases as the order of chemical reaction and heat generation parameters increase.

3) The concentration decreases as the thermal slip, reaction parameter, and Lewis number increase, whilst it increases as the order of the chemical reaction increase.

4) The heat and mass transfer rates reduce by increasing the thermal slip and the order of the chemical reaction parameters.

5) The generation and reaction parameters lead to the reduction of heat transfer rate, whilst they cause an increase in the mass transfer rate.

For further extensions of this paper, we can study various convective boundary conditions on the boundary layer free convection flow past a horizontal plate embedded in a porous medium filled by a nano-fluid containing different types of nanoparticles.

Acknowledgments

The authors are grateful to the reviewers for their valuable comments and suggestions. This work was supported and funded by Kuwait University Research Grant No. [SM02/20].

Conflict of interest

The authors declare no conflict of interest in this paper.

References

1. D. A. Nield, A. Bejan, *Convection in Porous Media*, 3nd edition, Springer-Verlag, 2006.
2. I. Pop, D. B. Ingham, *Convective Heat Transfer: Mathematical and Computational Modeling of Viscous Fluids and Porous Media*, Pergamon, 2001.
3. K. Vafai, *Handbook of Porous Media*, 2nd edition, Taylor Francis, New York, 2005.
4. M. V. Krishna, B. V. Swarnalathamma, A. J. Chamkha, Investigations of soret, joule and hall effects on MHD rotating mixed convective flow past an infinite vertical porous plate, *J. Ocean Eng. Sci.*, **4** (2019), 263–275.
5. D. B. Ingham, I. Pop, *Transport Phenomena in Porous Media III, Elsevie*r, Oxford, 2005.
6. K. Vafai, *Porous Media: Applications in Biological Systems and Biotechnology*, CRC Press, Boca Raton, 2010.
7. D. J. Pradeep, M. M. Noel, A finite horizon Markov decision process based reinforcement learning control of a rapid thermal processing system, *J. Process Control*, **68** (2018), 218–225.
8. P. Vadasz, *Emerging Topics in Heat and Mass Transfer in Porous Media*, Springer Netherlands, 2008.
9. S. U. S. Choi, Enhancing thermal conductivity of fluids with nanoparticles, *ASME Fed.*, **66** (1995), 99–105.
10. S. U. S. Choi, Z. G. Zhang, W. Yu, F. E. Lockwood, E. A Grulke, Anomalous thermal conductivity enhancement in nanotube suspensions, *Appl. Phys. Lett.*, **79** (2001), 2252–2254.
11. S. Lee, S. U. S. Choi, S. Li, J. A. Eastman, Measuring thermal conductivity of fluids containing oxide nanoparticles, *J. Heat Transf.*, **121** (1999), 280–289.
12. W. Bu-Xuan, L. P. Zhou, X. F. Peng, A fractal model for predicting the effective thermal conductivity of liquid with suspension of nanoparticles, *Int. J. Heat Mass Transf.*, **46** (2003), 2665–2672.
13. J. Koo, C. Kleinstreuer, A new thermal conductivity model for nanofluids, *J. Nanopart. Res.*, **6** (2004), 577–588.

14. B. Ghasemi, S. M. Aminossadati, Natural convection heat transfer in an inclined enclosure filled with a water-CuO nanofluid, *Numer. Heat Trans. A: App.*, **55** (2009), 807–823.
15. L. Godson, B. Raja, D. Mohan Lal, S. Wongwises, Enhancement of heat transfer using nanofluids –An overview, *Renew. Sustain. Energy Rev.*, **14** (2010), 629–641.
16. D. A. Nield, A. V. Kuznetsov, The Cheng-Minkowycz problem for natural convective boundary layer flow in a porous medium saturated by a nanofluid, *Int. J. Heat Mass Trans.*, **52** (2009), 5792–5795.
17. D. A. Nield, A. V. Kuznetsov, Thermal instability in a porous medium layer saturated by a nanofluid, *Int. J. Heat Mass Trans.*, **52** (2009), 5796–5801.
18. P. Cheng, W. J. Minkowycz, Free convection about a vertical flat plate embedded in a porous medium with application to heat transfer from a dike, *J. Geophys. Res.*, **82** (1977), 2040–2044.
19. R. S. R. Gorla, A. Chamkha, Natural convective boundary layer flow over a horizontal plate embedded in a porous medium saturated with a nanofluid, *J. Mod. Phys.*, **2** (2011), 62–71.
20. M. A. A. Hamad, M. Ferdows, Similarity solution of boundary layer stagnation flow towards a heated porous stretching sheet saturated with a nanofluid with heat absorption/generation and suction/blowing: a lie group analysis, *Commun. Nonlinear Sci. Numer. Simul.*, **17** (2012), 132–140.
21. S. Ahmad, I. Pop, Mixed convection boundary layer flow from a vertical flat plate embedded in a porous medium filled with nanofluids, *Int. Commun. Heat Mass Trans.*, **37** (2010), 987–991.
22. N. Arifin, R. Nazar, I. Pop, Free and mixed convection boundary layer flow past a horizontal surface embedded in a porous medium filled with a nanofluid, *J. Thermophys. Heat Trans.*, **26** (2012), 375–382.
23. L. V. Ovsiannikov, *Group Analysis of Differential Equations*, Academic Press, New York, 1982.
24. N. H. Ibragimov, *Elementary Lie Group Analysis and Ordinary Differential Equations*, Wiley, New York, 1999.
25. G. W. Bluman, S. Kumei, *Symmetries and Differential Equations*, Springer-Verlag, New York, 1989.
26. M. V. Krishna, M. G. Reddy, A. J. Chamkha, Heat and mass transfer on MHD free convective flow over an infinite non-conducting vertical flat porous plate, *Int. J. Fluid Mech. Res.*, **46** (2019), 1–25.
27. M. V. Krishna, Hall and ion slip impacts on unsteady MHD free convective rotating flow of Jeffreys fluid with ramped wall temperature, *Int. Commun. Heat Mass Trans.*, **119** (2020), 104927.
28. M. V. Krishna, A. J. Chamkha, Hall and ion slip effects on magneto-hydrodynamic convective rotating flow of Jeffreys fluid over an impulsively moving vertical plate embedded in a saturated porous medium with Ramped wall temperature, *Numer. Methods Partial D. E.*, **37** (2021), 2150–2177.
29. M. V. Krishna, A. J. Chamkha, Hall and ion slip effects on MHD rotating boundary layer flow of nanofluid past an infinite vertical plate embedded in a porous medium, *Results Phys.*, **15** (2019), 102652.
30. M. V. Krishna, N. A. Ahamad, A. J. Chamkha, Hall and ion slip effects on unsteady MHD free convective rotating flow through a saturated porous medium over an exponential accelerated plate, *Alex. Eng. J.*, **59** (2020), 565–577.
31. M. V. Krishna, N. A. Ahamad, A. J. Chamkha, Radiation absorption on MHD convective flow of nanofluids through vertically travelling absorbent plate, *Ain Shams Eng. J.*, **11** (2021), 1–14.

32. A. B. Patil, P. P. Humane, V. S. Patil, G. R. Rajput, MHD Prandtl nanofluid flow due to convectively heated stretching sheet below the control of chemical reaction with thermal radiation, *Int. J. Ambient Energy*, (2021), 1–13.
33. M. Yürüsoy, M. Pakdemirli, Symmetry reductions of unsteady three-dimensional boundary layers of some non-Newtonian fluids, *Int. J. Eng. Sci.*, **35** (1997), 731–740.
34. M. Yürüsoy, M. Pakdemirli, Group classification of a non-Newtonian fluid model using classical approach and equivalence transformations, *Int. J. Nonlinear Mech.*, **34** (1999), 341–346.
35. R. Abdul-Kahar, R. Kandasamy, I. Muhaimin, Scaling group transformation for boundary layer flow of a nanofluid past a porous vertical stretching surface in the presence of chemical reaction with heat radiation, *Comput. Fluids*, **52** (2011), 15–21.
36. M. A. A. Hamad, M. J. Uddin, A. I. M. Ismail, Investigation of combined heat and mass transfer by Lie group analysis with variable diffusivity taking into account hydrodynamic slip and thermal convective boundary conditions, *Int. J. Heat Mass Trans.*, **55** (2012), 1355–1362.
37. V. S. Patil, A. B. Patil, S. Ganesh, P. P. Humane, N. S. Patil, Unsteady MHD flow of a nano powell-eyring fluid near stagnation point past a convectively heated stretching sheet in the existence of chemical reaction with thermal radiation, *Mater. Today: Proc.*, **44** (2021), 3767–3776.
38. A. A. Afify, N. S. Elgazery, Lie group analysis for the effects of chemical reaction on MHD stagnation-point flow of heat and mass transfer towards a heated porous stretching sheet with suction or injection, *Nonlinear Anal-Model.*, **17** (2012), 1–15.
39. M. Ferdows, M. J. Uddin, A. A. Afify, Scaling group transformation for MHD boundary layer free convective heat and mass transfer flow past a convectively heated nonlinear radiating stretching sheet, *Int. J. Heat Mass Trans.*, **56** (2013), 181–187.
40. M. J. Uddin, M. Ferdows, M. M. Rashidi, A. B. Parsa, Group analysis and numerical solution of slip flow of a nanofluid in porous media with heat transfer, *Progr. Comput. Fluid Dynam. Int. J.*, **16** (2016), 190–200.
41. M. J. Uddin, W.A. Khan, A. I. M. Ismail, Free convection boundary layer flow from a heated upward facing horizontal flat plate embedded in a porous medium filled by a nanofluid with convective boundary condition, *Transp. Porous Media*, **92** (2012), 867–881.
42. M. Rashidi, E. Momoniat, M. Ferdows, A. Basiriparsa, Lie group solution for free convective flow of a nanofluid past a chemically reacting horizontal plate on a porous media, *Math. Prob. Eng.*, (2014), 239082.
43. A. Aziz, W. A. Khan, I. Pop, Free convection boundary layer flow past a horizontal flat plate embedded in a porous medium filled by a nanofluid containing gyrotactic microorganisms, *Int. J. Therm. Sci.*, **56** (2012), 48–57.
44. W. A. Khan, I. Pop, Free convection boundary layer flow past a horizontal flat plate embedded in a porous medium filled with a nanofluid, *J. Heat Transf.*, **133** (2011), 094501.
45. J. Buongiorno, Convective transport in nanofluids, *J. Heat Transf.*, **128** (2006), 240–250.
46. D. A. Nield, A. V. Kuznetsov, The Cheng–Minkowycz problem for the double-diffusive natural convective boundary layer flow in a porous medium saturated by a nanofluid, *Int. J. Heat Mass Trans.*, **54** (2011), 374–378.
47. T. Tapanidis, G. Tsagas, H. P. Mazumdar, Application of scaling group of transformations to viscoelastic second grade fluid flow, *Nonlinear Funct. Anal. Appl.*, **8** (2003), 345–350.
48. S. Mukhopadhyay, G. C. Layek, Effects of variable fluid viscosity on flow past a heated stretching sheet embedded in a porous medium in presence of heat source/sink, *Meccanica*, **47** (2012), 863–876.

49. A. G. Hansen, *Similarity Analysis of Boundary Value Problems in Engineering*, Prentice Hall, New Jersey, 1964.
50. W. F. Ames, *Nonlinear Partial Differential Equations in Engineering*, Academic Press, New York, 1972.
51. P. Cheng, I. D. Chang, Buoyancy induced flows in a saturated porous medium adjacent to impermeable horizontal surfaces, *Int. J. Heat Mass Trans.*, **19** (1976), 1267–1272.
52. A. Aziz, A similarity solution for laminar thermal boundary layer over a flat plate with a convective surface boundary condition, *Commun. Nonlinear Sci. Numer. Simul.*, **14** (2009), 1064–1068.
53. R. E. White, V. R. Subramanian, *Computational Methods in Chemical Engineering with Maple*, Springer-Verlag, 2010.
54. A. Pantokratoras, Study of MHD boundary layer flow over a heated stretching sheet with variable viscosity: a numerical reinvestigation, *Int. J. Heat Mass Trans.*, **51** (2008), 104–110.
55. A. Alsaedi, M. Awais, T. Hayat, Effects of heat generation/absorption on stagnation point flow of nanofluid over a surface with convective boundary conditions, *Commun. Nonlinear Sci. Numer. Simul.*, **17** (2012), 4210–4223.